THE ASTROPHYSICAL JOURNAL, 546:1075–1085, 2001 January 10

DETECTION OF A SERIES OF X-RAY DIPS ASSOCIATED WITH A RADIO FLARE IN GRS 1915+105

S. NAIK,[1] P. C. AGRAWAL,[1] A. R. RAO,[1] B. PAUL,[1,2] S. SEETHA,[3] AND K. KASTURIRANGAN[3]

Received 2000 February 22; accepted 2000 August 31

ABSTRACT

We report the detection of a series of X-ray dips in the Galactic black hole candidate GRS 1915+105 during 1999 June 6–17 from observations carried out with the pointed proportional counters of the Indian X-ray Astronomy Experiment on board the *Indian Remote Sensing Satellite* (*IRS*-P3). The observations were made after the source made a transition from a steady low-hard state to a chaotic state, which occurred within a few hours. Dips of about 20–160 s in duration were observed on most of the days. The X-ray emission outside the dips shows a quasi-periodic oscillation (QPO) at ~4 Hz that has characteristics similar to the ubiquitous 0.5–10 Hz QPO seen during the low-hard state of the source. During the onset of dips this QPO is absent, and, also, the energy spectrum is soft and the variability is low compared to the nondip periods. These features gradually reappear as the dip recovers. The onset of the occurrence of a large number of such dips followed the start of a huge radio flare of strength 0.48 Jy (at 2.25 GHz). We interpret these dips as the cause for mass ejection due to the evacuation of matter from an accretion disk around the black hole. We propose that a superposition of a large number of such dip events produces a huge radio jet in GRS 1915+105.

Subject headings: accretion, accretion disks — binaries: close — black hole physics — stars: individual (GRS 1915+105) — X-rays: bursts — X-rays: stars

1. INTRODUCTION

The X-ray transient source GRS 1915+105 was discovered by Castro-Tirado, Brandt, & Lund (1992) with the WATCH all-sky X-ray monitor on board the *Granat* satellite. The source has been exhibiting a wide variety of temporal variability in its X-ray and radio emission. GRS 1915+105, the first Galactic superluminal radio source, has characteristics of a microquasar and is located at a distance of about 12.5 ± 1.5 kpc (Mirabel & Rodríguez 1994).

Besides the chaotic variability, narrow quasi-periodic oscillations (QPOs) at centroid frequencies in the range of 0.001–10 Hz were discovered in the X-ray emission from the source using the Indian X-ray Astronomy Experiment (IXAE; Agrawal et al. 1996) and the *Rossi X-Ray Timing Explorer* (*RXTE*; Morgan & Remillard 1996). A QPO at a centroid frequency of 67 Hz that does not change with time was also detected in this source in the *RXTE* observations. It has been suggested that it is related to the innermost stable orbit in the accretion disk of the source. Chen, Swank, & Taam (1997) found that the intensity-dependent narrow QPOs are a characteristic feature of the hard branch, and they are absent in the soft branch, which corresponds to the very high state similar to those of other black hole candidates. Trudolyubov, Churazov, & Gilfanov (1999) studied the 1996/1997 low-luminosity state and transitions of states using the *RXTE* data. They found a strong correlation between the QPO centroid frequency and spectral and timing parameters similar to the one detected in other Galactic black hole candidates in the intermediate state. Muno, Morgan, & Remillard (1999) sampled the *RXTE* data over a wide range of properties and found that the 0.5–10 Hz QPOs are correlated with the temperature of the accretion disk. From study of the source's behavior, they distinguish two different states of the source: the spectrally hard state, dominated by a power-law component when the QPOs are present, and the soft state, dominated by thermal emission when the QPOs are absent.

Paul et al. (1998) detected quasi-periodic bursts with a period of about 45 s using the IXAE data obtained in 1997 June–August and interpreted the slow rise and fast decay of bursts as evidence of matter disappearing into the event horizon of the black hole. Yadav et al. (1999) made a systematic analysis of these bursts and classified them into regular, irregular, and quasi-regular based on the burst duration and recurrence time. They found that the bursts recur at a mean time of 20–150 s, and they suggested that the irregular long-duration bursts (recurrence time ~120 s), during which the spectrum becomes harder and harder as the burst progresses and becomes hardest at the end of the decay, are characteristic of the change of state of the source. They calculated the rise time and the decay time for these bursts to be of the order of a few seconds (~10 s). The back and forth switching of the state of the source from a low hard to a high soft state within a timescale of a few seconds is explained by invoking the appearance and disappearance of the advective disk over its viscous timescale. These irregular bursts were also quasi-simultaneously observed by Belloni et al. (1997), who interpreted them as repeated filling and evacuation of inner accretion disc.

Simultaneous X-ray and infrared observations of the source established a close link between the nonthermal infrared emission and the X-ray emission from the accretion disk (Eikenberry et al. 1998). They found that the X-ray properties showed a drastic change coincident with the occurrence of the IR and radio flares. Similar episodes of X-ray and radio flares were detected by Feroci et al. (1999) using the *BeppoSAX* satellite. From the spectral analysis of the X-ray data, they found evidence for a temporary disappearance and subsequent restoration of the inner accretion disk during the flare. Such simultaneous multiwavelength

[1] Tata Institute of Fundamental Research, Homi Bhabha Road, Mumbai 400 005, India; sachi@tifr.res.in, pagrawal@tifr.res.in, arrao@tifr.res.in, bpaul@tifr.res.in.

[2] Institute of Space and Astronautical Science, 3-1-1 Yoshinodai, Sagamihara, Kanagawa 229-8510, Japan.

[3] ISRO Satellite Center, Airport Road, Vimanapura P.O., Bangalore 560-017, India.

TABLE 1

LOG OF X-RAY OBSERVATIONS OF GRS 1905+105 WITH IXAE

Observation Date (1999)	Start Time (UT)	End Time (UT)	Count Rate	Source Intensity (crab)	Duration of Dips (s)
Jun 6	17:01	17:18	565	0.686	...
Jun 7	17:31	17:48	513	0.623	...
Jun 8	11:02	11:15	944	1.146	...
	13:45	14:03	670	0.814	...
	15:28	15:45	541	0.657	125
	17:09	17:20	1124	1.365	140, 40
	18:54	19:06	1718	2.086	160
Jun 9	13:24	13:42	671	0.814	145
	15:07	15:24	399	0.485	...
	16:48	17:05	1291	1.568	85, 60
	18:28	18:43	1036	1.258	...
Jun 10.....	11:21	11:39	540	0.656	...
	13:03	13:21	320	0.389	110, 50, 40, 30
	16:40	16:44	1708	2.074	120
	18:07	18:24	688	0.835	110
Jun 11.....	12:47	12:59	1809	2.196	...
	14:23	14:41	1416	1.719	130, 40
	16:06	16:22	794	0.964	...
	17:46	18:04	1478	1.794	120
Jun 12.....	12:20	12:37	527	0.640	10 dips (20 –40 s)
	19:13	19:23	1048	1.272	7 dips (20–40 s)
Jun 13.....	13:41	13:59	295	0.358	160, 40, 30, 20
	17:06	17:23	1044	1.267	40, 30, 30
	18:49	19:01	732	0.889	...
Jun 14.....	11:38	13:55	306	0.372	120, 40, 20, 20
	16:45	17:01	1094	1.328	100, 30, 20, 40
	18:23	18:40	876	1.063	30, 20, 40, 30
Jun 15.....	12:59	13:16	432	0.524	120, 20, 20, 20
	14:41	14:57	503	0.611	5 dips (20–30 s)
	16:27	16:40	376	0.457	...
	18:01	18:19	580	0.704	3 dips (20–30 s)
Jun 16.....	15:59	16:21	305	0.37	...
	17:41	18:00	1335	1.62	...
Jun 17.....	17:18	17:40	748	0.908	...
	18:49	19:00	1347	1.635	...

observations establish the disk-jet connection in GRS 1915+105. These observations, however, pertain to jet emission that can be termed as "baby jets" (Eikenberry et al. 1998) from consideration of energy. On the other hand, the accretion-disk phenomena giving rise to superluminal jets are not established very clearly. Harmon et al. (1997) found an anticorrelation between the decrease in the hard X-ray flux (obtained from BATSE with a time resolution of $\sim$1 day) from the accretion disk and the subsequent jet production. Fender et al. (1999) worked back the time of occurrence of superluminally moving jets and found rapid (20–30 minute) radio oscillations during the beginning of such jets. Though they attempted to associate these oscillations with the X-ray oscillations detected by Belloni et al. (1997), there are no simultaneous high time-resolution observations in the radio and X-ray wave bands during huge radio flares responsible for superluminal jets. Though there is some indication of association between radio and X-ray emission based on low time-resolution observations (*RXTE*/ASM and GBI), detailed quantitative association between the two is not very conclusive. Hence, we can conclude that the disk-jet connection for jets with superluminal motion is indirect at best.

In this paper we report the detection of multiple X-ray dips interpreted as "disk-evacuation" events that are similar in nature to the "baby jet" X-ray events (Eikenberry et al. 1998; Mirabel et al. 1998). These events started during the transition of the source state from a steady low hard state with the X-ray flux at 0.62 crab at 1999 June 7 17.79 UT to a chaotic state with a flux of 1.46 crab at 19.22 UT. A simultaneous increase in radio flux was seen at 2.25 GHz from 0.029 Jy at 1999 June 7 10.94 UT to 0.478 Jy on 1999 June 8 05.54 UT (from the public domain data from the NSF-NRAO-NASA Green Bank Interferometer). The presence of multiple dips in the X-ray light curve after the transition of the state when a radio flare also occurred suggests the presence of a "disk-evacuation" process in the inner accretion disk of GRS 1915+105.

2. INSTRUMENT AND OBSERVATIONS

The X-ray observations of GRS 1915+105 were carried out with the pointed proportional counters (PPCs) of IXAE on board the Indian satellite *IRS*-P3. The IXAE includes three co-aligned and identical multiwire, multilayer proportional counters filled with a gas mixture of 90% argon and 10% methane at a pressure of 800 torr with a total effective area of 1200 cm^2, covering the 2–18 keV energy range with an average detection efficiency of about 60% at 6 keV. The accepted X-ray events are stored in counters in 2–6 keV and 2–18 keV bands for the top layer, 2–18 keV

bands for the middle layer, greater than 18 keV (ULD counts) for all layers, and greater than 2 keV counts from the veto layers. For a detailed description of the PPCs, refer to Agrawal (1998) and Rao et al. (1998).

The *IRS*-P3 satellite is in a circular orbit at an altitude of 830 km and an inclination of 98°. Pointing toward any particular source is done by using a star tracker with an accuracy of $\leq 0.^{\circ}1$. The useful observation time is limited to five of the 14 orbits outside the South Atlantic Anomaly (SAA) region to the latitude band of 30° South to 50° North to avoid the charge particle background. The high voltage to the detectors is reduced when the satellite enters the SAA region and the data acquisition is stopped.

Background observations were made at the end of the source observation by pointing the PPCs to a source-free region in the sky close to the target source since the simultaneous background observation is not possible because of the co-alignment of the PPCs. The source GRS 1915+105 was observed from 1999 June 6–15 with 1 s time-integration mode and June 16–17 in 0.1 s time bin, for a useful period of 37,740 s. The log of the observations is given in Table 1.

3. ANALYSIS AND RESULTS

The data, corrected for background and pointing offset for PPC-1 and PPC-3, were added to construct the X-ray light curve for GRS 1915+105. The dead-time correction is not done since it is less than 1% for each PPC, since the event processing time for each PPCs is about 20 μs. The X-ray light curve for the source in the energy range of 2–18 keV for all the observations with the PPCs averaged over each orbit is shown in Figure 1 (*top panel*). Also seen in the figure are 1.3–12.2 keV energy range light curves obtained with the *RXTE*/ASM (*middle panel*) and the radio flux at the frequency 2.25 GHz (*bottom panel*). The radio observations were taken from the public domain data from the NSF-NRAO-NASA Green Bank Interferometer.

As can be deduced from the low-resolution ASM and GBI data, the source was in a steady low hard state from June 2 to June 7 (MJD 51,331–51,336). It made a transition to a "chaotic state" in a very short time, which is very different from the slow transition (about three months) of the source in 1997 May to July (Trudolyubov et al. 1999). The source count rate increased from about 53 ASM counts s^{-1} on MJD 51,336.5 (June 7 12.00 UT) to 109.4 ASM counts s^{-1} on MJD 51,336.8 (June 7 19.2 UT). The onset of X-ray activity is further constrained by the PPC observations on June 7 17.50 UT, when the source showed steady behavior. Hence, we can conclude that there was an abrupt change in the X-ray emission characteristics in less than 1.7 hr. From the radio light curve of the source, a sharp peak is clearly visible on MJD 51,337 (June 8), on the same day when the source showed the X-ray transition as seen from the *RXTE*/ASM light curve. The onset of the radio flaring event is between June 7 10.94 UT and June 8 05.54 UT. After the radio peak, on MJD 51,337, the flux decayed slowly over next 5 days. The exponential decay time of the radio flare is estimated to be 2.8 days. Though the low time-resolution X-ray light curve appears like a flaring event, a closer examination of the high-resolution data reveals that variations of much shorter duration are also

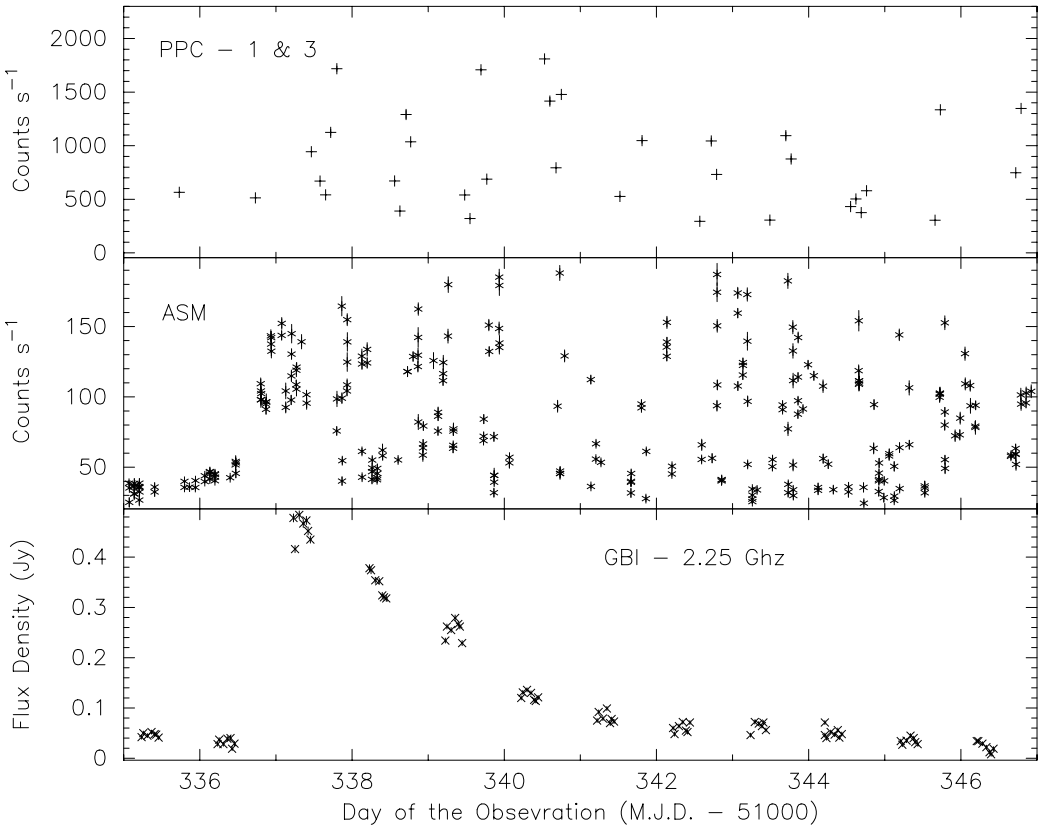

FIG. 1.—X-ray light curve for GRS 1915+105 with the PPCs (averaged over each orbit) in the energy range of 2–18 keV, with *RXTE*/ASM in the range of 1.3–12.2 keV, and radio flux at 2.25 GHz with NSF-NRAO-NASA Green Bank Interferometer, during the observation of the source by the PPCs in IXAE in 1999 June.

present, as indicated by a factor of 4–5 variations over a few days within a span of a few hundred seconds in a series of dips.

The light curves for some of the individual observations of the source with the PPCs are shown in Figures 2 and 3. No bursts or dips are seen in the X-ray light curves of 1999 June 6 and 7 (MJD 51,335 and 51,336) when the source was in a low hard state. From 1999 June 8 onward, various types of dips of duration in the range of 20–160 s are seen in most of the observations, as shown in Figures 2 and 3. During the dips the X-ray flux decreases by a factor of about 3 within about 5 s, remains low for 20–160 s, and then slowly recovers to the maximum. The short-term variability in the X-ray light curves decreases during the dip. The duration of the dips is not constant in all the observations. In some of the observations short-period dips of 20–60 s duration are observed after the occurrence of long dip with duration of more than 100 s. Toward the end of the observation long duration dips lasting for more than 100 s are not seen, but larger numbers of shorter duration dips are observed. A summary of the duration of dips observed in the light curves of the source is given in Table 1.

The first three panels of Figure 4 show one of the dips observed during the PPC observations in 2–18 keV, 2–6 keV, and 6–18 keV energy ranges, co-added by matching the falling part of the dips. In the figure the sharp decrease in the X-ray flux to almost one-third of its original value followed by a slow recovery is clearly seen. We have calculated the rise time and decay time for the dips by fitting exponentials to the light curve. The values are found to be about 110 and 7 s, respectively. The hardness ratio (counts in 6–18 keV energy range to counts in 2–6 keV energy range) for the same observation is shown in the fourth panel of the figure. It is seen from the figure that during the dips the spectrum (hardness ratio) of the source is soft. The bottom panel in Figure 4 shows the rms variation in the source calculated for three successive data points in the light curve for the 2–18 keV energy range during the dip and nondip regions. There is a sharp decrease in the rms value at the beginning of the dip, which recovers gradually as the flux increases.

The hardness ratio is computed for all the PPC observations. It is found that during the dips, the value of the hardness ratio is less in comparison to the nondip regions for all the observation, which indicates that the spectrum of the source is soft during the dips. There is no significant change in the value of the hardness ratio averaged over each orbit. The timing behavior of the source was studied by taking the Fourier transform of 1 and 0.1 s resolution mode data. From the power density spectrum (PDS) constructed from 0.1 s time mode data of June 17, narrow QPOs are detected at 4.5 Hz, as shown in Figure 5, along with the 1 s bin light curve. From the figure it is clear that the QPOs are present in the source when there are no dips in the light curve. Since the time resolution is limited to 1 s for most of the observations, we could not study in detail the QPOs in the frequency range of 1–10 Hz during those periods when the dips were present.

In Table 2 we summarize various properties of the source during the dip and nondip periods. The average count rate during the dips is about one-half or one-third of the count rate during the nondip regions. The values of the hardness

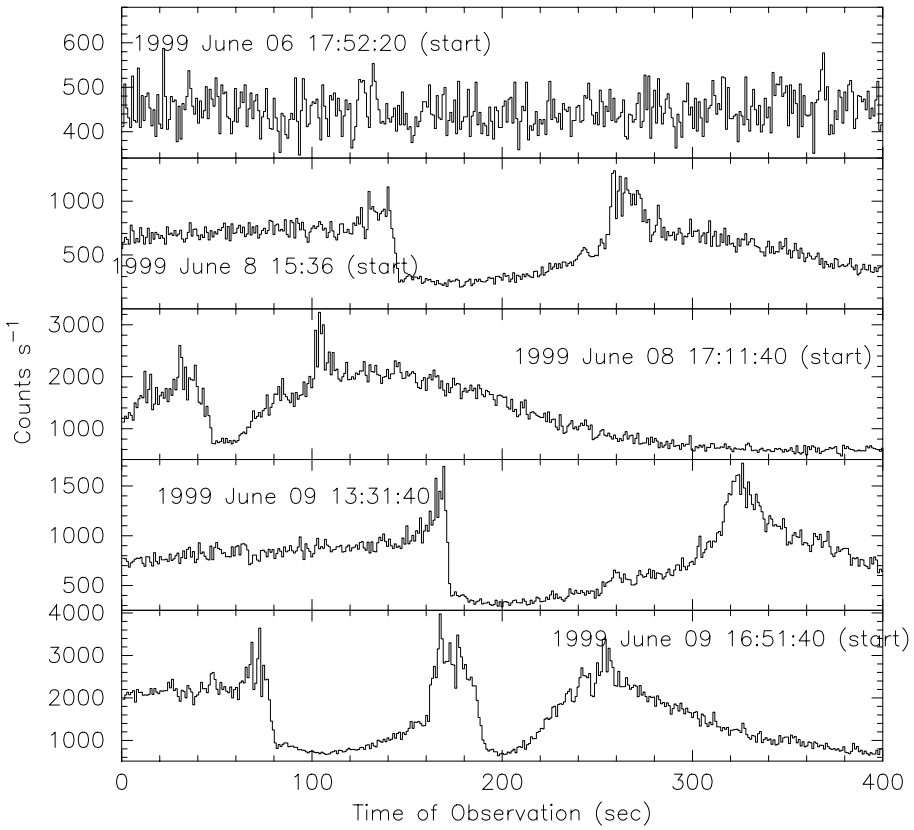

FIG. 2.—Light curves of GRS 1915+105 with the PPCs with 1 s bin size in the energy range of 2–18 keV for June 6, 8, and 9. The presence of different types of dips with different periods in the light curve of the source are shown.

TABLE 2

PROPERTIES OF GRS 1905+105 DURING DIP AND NONDIP PERIODS

Observation Date (1999)	Time (UT)	Count Rate during Dip	Count Rate during Nondip	rms during Dip	rms during Nondip	Average HR during Dip	Average HR during Nondip
Jun 8	15:36	253.2	713.5	13.9	28.6	...	...
	17:09	781.5	1540.6	2.54	8.69	...	...
	18:54	854.2	1842	2.5	5.95	...	...
Jun 9	13:24	361.3	791.6	2.32	3.27	1.8	2.1
	16:48	782.2	2214.8	2.58	5.26	1.63	1.95
Jun 10.....	13:03	198.1	555.77	1.38	4.14	1.8	2.13
	16:39	409.3	814.1	1.14	2.10	1.75	1.92
	18:09	387.8	816.3	1.26	3.17	1.67	1.865
Jun 11.....	14:23	725.3	2029.2	1.97	4.52	...	...
	17:46	257.1	615.0	1.91	1.77	...	...
Jun 12.....	12:20	267.2	635.8	2.6	2.36	1.9	2.1
	19:13	724.3	1450.8	1.78	3.89	1.6	1.98
Jun 13.....	13:41	177.9	235.9	1.81	2.32	1.95	1.98
	17:06	691.6	1769.9	2.75	3.98	1.75	2.04
Jun 14.....	11:39	221.4	526.6	2.2	4.45	1.98	2.52
	16:44	721.2	1434	1.95	4.79	1.74	2.18
	18:23	650.5	1563.2	2.64	5.8	1.75	2.06
Jun 15.....	12:59	400.5	784.7	1.79	2.42	1.89	2.40
	14:41	286.3	462.4	1.11	2.07	1.65	1.95

NOTE.—HR stands for hardness ratio.

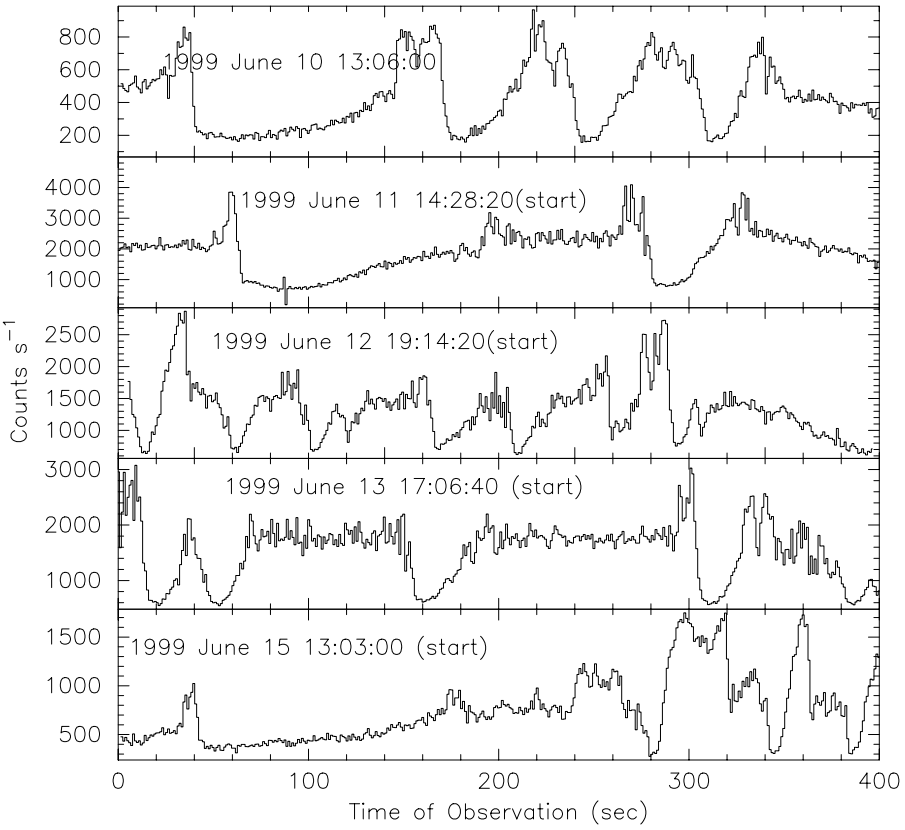

FIG. 3.—Same as Fig. 2 for June 10, 11, 12, 13, 14, and 15

ratio and rms variations of the source are always smaller for the dip periods compared to the nondip periods.

All the above properties of the source during the nondip and dip regions are also seen in the publicly available *RXTE*/PCA data on 1999 June 8. The *RXTE*/PCA public archive contains only one observation during the radio flare (from June 8 to June 13), and we have analyzed this data to substantiate the properties of the dips. The first dip in the X-ray band detected with the PPCs (Fig. 2, *second panel*) was also seen with *RXTE*/PCA at the same time. Figure 6 shows the X-ray light curve of the *RXTE*/PCA data in the energy range of 2–13 keV (*upper panel*) and the hardness ratio (count rate in the 5–13 keV energy range to count rate in the 2–5 keV energy range, *lower panel*) for the source. The PDS for the source for the different regions, i.e., regions during the dips and during the absence of dips, is shown in Figure 7. The first, third, and fifth panels in the figure represent the PDS during the absence of the dips, and the second and fourth panels show the PDS during the dips. A narrow QPO peak at a centroid frequency in the range of 4–6 Hz is seen in the nondip regions, which is absent in the dips. The spectrum during the dips is softer in comparison to the nondip regions. These properties are consistent with the PPC observations.

The dips detected in the X-ray light curves with the PPCs are similar to the dips that occurred after the spike in the X-ray light curve, observed on 1997 May 15 and September 9 (Markwardt, Swank, & Taam 1999; Mirabel et al. 1998), which is described as the "quiet" state by Markwardt et al. (1999). The properties of the source during this state are similar to those found during the dips observed in 1999 June with the PPCs.

During the multiwavelength observation of the source carried out on 1997 May 15 and September 9, it was found that an X-ray event is followed by nonthermal infrared and radio flares. Here we estimate whether a series of minijets similar to those observed on 1997 May 15 (Mirabel et al. 1998) associated with the dips can account for the huge radio flare. From the simultaneous observation of the source in X-ray, IR, and radio, Mirabel et al. (1998) estimated the value of spectral index of the relativistic electrons by applying the van der Laan (1966) model and derived a relation for the observed maximum flux density (S_λ) at a given wavelength λ and the time since the ejection to reach the maximum flux at a particular wavelength (t_λ), given by

$$S_\lambda \propto \lambda^{-(7p+3)/(4p+6)} \quad (1)$$

$$t_\lambda \propto \lambda^{(p+4)/(4p+6)} . \quad (2)$$

They found the value of spectral index $p \simeq 0$ by using the observed maximum flux density at 3.6 and 6 cm during the burst observed on 1997 May 15. They determined the time for $t_{6\ \mathrm{cm}} \simeq 0.9$ hr and $t_{3.6\ \mathrm{cm}} \simeq 0.65$ hr. Using these parameters, we estimate the peak flux at 2.25 GHz ($\lambda = 13.3$ cm) as 26.5 mJy and $t_{13.6\ \mathrm{cm}}$ as 1.6 hr. Assuming the time profile of the radio emission as seen by Mirabel et al. (1998), we estimate the total radio emission at 2.25 GHz ($\lambda = 13.3$ cm) in the radio miniflare corresponding to a dip in X-ray flux as

$$F_{13.3} \simeq 40\ \mathrm{mJy\ hr^{-1}} . \quad (3)$$

The total radio emission at 2.25 GHz during the 1999 June flaring is estimated by integrating the radio profile (for 6 days) by fitting an exponential to the decay phase of the light curve. If the total radio emission in the flare observed

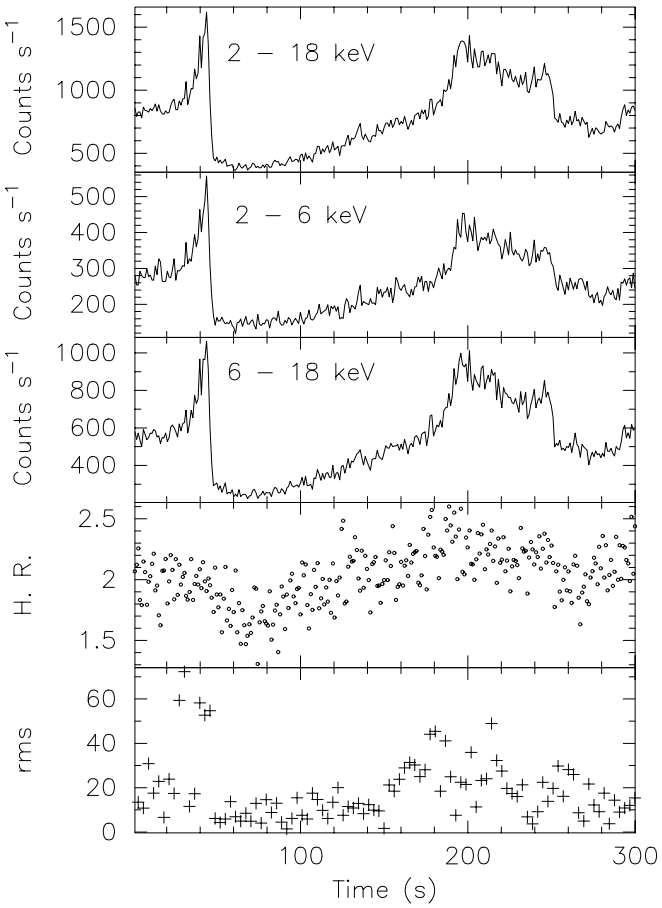

FIG. 4.—Light curves of GRS 1915+105 during the dips observed with the PPCs with 1 s bin size in the energy range of 2–18 keV, 2–6 keV, and 6–18 keV. The dip is identical in shape in all the energy ranges. The hardness ratio (HR) is plotted in the fourth panel of the figure, which indicates the soft nature of the spectrum during the dips. The lower panel shows the variation in the rms of the source during the dip and nondip regions.

in 1999 June is a superposition of such miniflares, we can calculate the approximate number of dips in the X-ray light curve required to produce the radio flare as 720. If miniflares in the radio are associated with the dips in the X-ray, this gives a rate of one dip in 12 minutes (in PPC).

4. DISCUSSION

Galactic superluminal sources are ideal astrophysical laboratories to probe in detail the connection between jets and accretion disks, ubiquitously thought to be present in quasars. There were several attempts in the past to isolate characteristics in the X-ray emission of these sources (assumed to be coming from an accretion disk) and relate them to the onset of jet emission. Also, evidence for a sudden mass-ejection event from the accretion disk is sought in the X-ray emission characteristics. Belloni et al. (1997) have discovered a series of outbursts in GRS 1915+105 that were attributed to "inner-disk" evacuation. They found that the source makes a transition to two intensity levels lasting from a few tens to a few hundred seconds with distinct and different inner disk radii (as obtained from spectral measurements), and they attributed this change to the disappearance of the inner disk due to thermal-viscous instabilities. Fender et al. (1999) made a detailed analysis of the superluminal jet-ejection events observed in GRS 1915+105 in 1997 October/November and detected continuous short-period (20–40 minute) radio oscillations shortly after the start of the jet emission. They proposed that these are indications of repeated ejection of the inner accretion disk, quite similar to the events seen in X-rays by Belloni et al. (1997). A causal connection between disk and jet was thus attempted.

Paul et al. (1998) and Yadav et al. (1999) have made a detailed study of such intensity variations using the data obtained with the IXAE and contemporaneous to the burst events reported by Belloni et al. (1997). They found that the source spectrum, i.e., the ratio between the count rate in the 6–18 keV energy range to count rate in the 2–6 keV energy range, was softer during the burst and harder during the quiescent phase. Yadav et al. (1999) concluded that the repeated intensity variation cannot be attributed to inner disk evacuation. This is due to the viscous timescale arguments as well to the fact that the two intensity states are quite similar to the low hard and high soft state of the source. They invoked the two-component accretion-flow model (TCAF) of Chakrabarti & Titarchuk (1995) to conclude that the rapid changes are due to the appearance and disappearance of advective disk covering the standard thin disk without any requirements of mass ejection. Further, these types of hard dips (with a transition time of a few seconds) are seen for almost a month in 1997 June (Yadav et al. 1999) when the radio emission was low. We estimate an average radio emission for this month as 8 mJy at 2.25 GHz using the GBI data. There was also no evidence for any flares (flux < 20 mJy at all times). Hence, the causal relationship between the disk instabilities and jet emission can be treated as not completely established.

In the next subsection we summarize the available X-ray and radio observations that indicate the disk-jet connections.

4.1. *Radio and X-Ray Emission in GRS 1915+105*

1. There are periods of long durations when both the radio as well as the X-ray emissions are low. One example is from 1997 January–March, when the X-ray flux was ~ 0.25 crab, and the 2.25 GHz radio flux was 10 mJy. These are classified as the radio-quiet hard state observations in Muno et al. (1999).

2. There are durations when the X-ray and radio flux are higher, which are classified as radio-loud hard steady state. They are also known to exhibit optically thick radio emission and referred to as the "plateau" state (1996 July–August, 1997 October). For the 1997 October "plateau" state, the X-ray flux is 0.50 crab, and the 2.25 GHz radio flux is 50 mJy. There is evidence for an AU-scale radio-jet observation in this state (Dhawan, Mirabel, & Rodríguez 2000).

3. The X-ray flux changes from the steady hard state to a flaring state at various timescales from a few hours (as seen in the present work) to a few months. During this time a variety of X-ray variations are seen.

3.1. The X-ray flux teeters between two intensity states in a short time (a few seconds) with a periodicity of 20–150 s. These are called "inner-disk oscillations" by Belloni et al. (1997) and "irregular and quasi-regular" bursts by Yadav et al. (1999). There is no evidence for enhanced radio emission during these events.

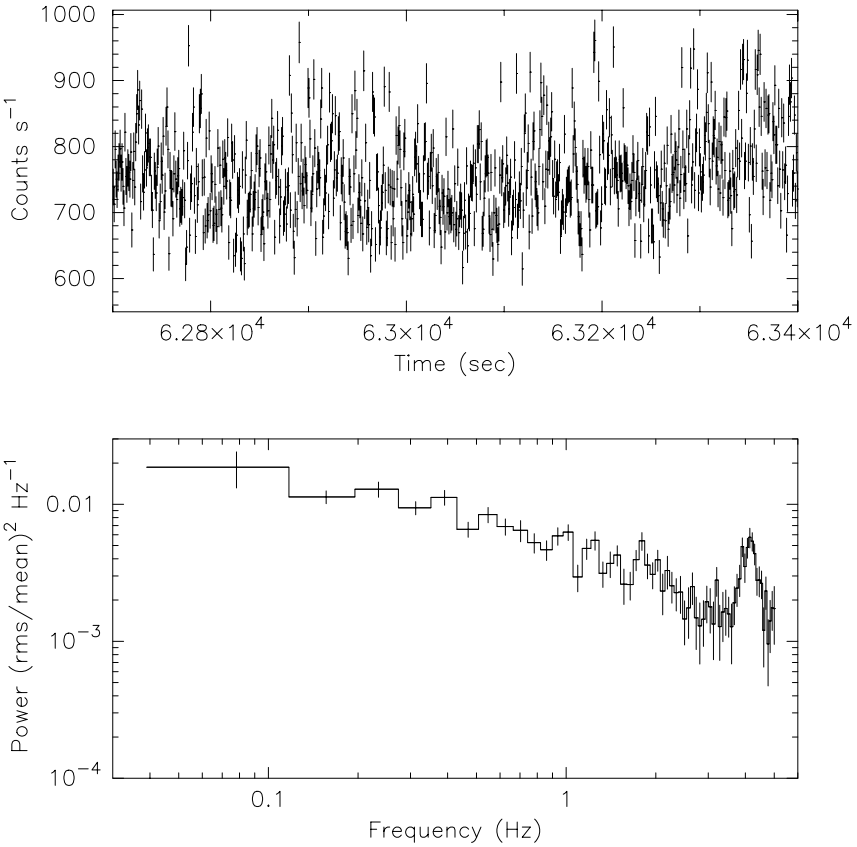

FIG. 5.—Light curve and PDS of GRS 1915+105 with the PPCs in the energy range 2–18 keV on 1999 June 17. The presence of a QPO peak at frequency 4.5 Hz is seen during the nondip period in the X-ray light curve.

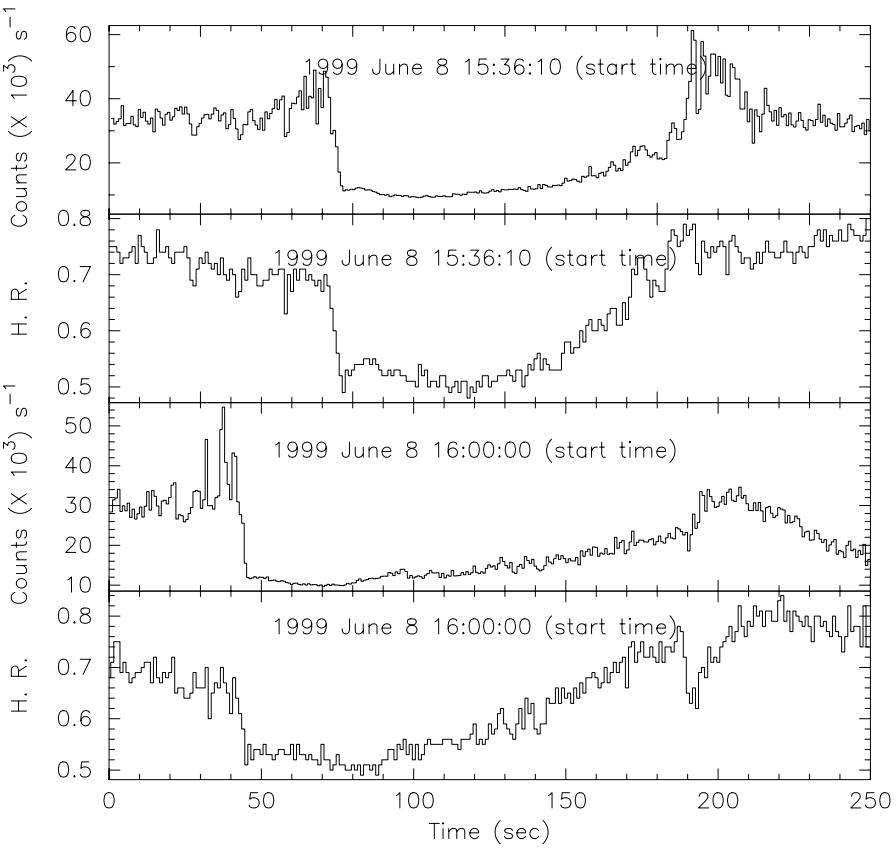

FIG. 6.—Light curve of GRS 1915+105 obtained with the *RXTE*/PCA data on MJD 51,337 in the 2–13 keV energy range with 0.8 s time bin is shown for two dips (*top panel* and *second panel from bottom*). The hardness ratio (HR) of the source, i.e., count rate in 5–13 keV energy range / count rate in 2–5 keV energy range, is also shown (*second panel from top* and *bottom panel*).

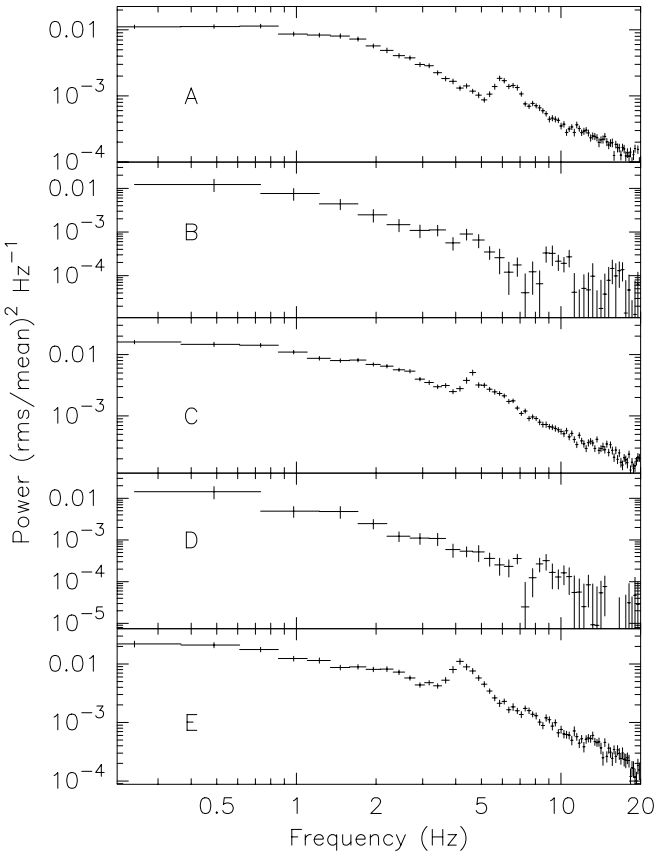

FIG. 7.—PDS of the source GRS 1915+105 in the energy range of 5–13 keV for different regions of the light curve. Panels A, C, and E represent the PDS during the nondip periods, i.e., earlier to the first dip, between the two dips and beyond the second dip, respectively, as seen with the *RXTE*/PCA on 1999 June 8. Panels B and D represent the PDS during the dip periods in the light curve. The figure shows the presence of QPOs in the frequency range of 4–6 Hz during the nondip regions that are absent during the dips.

3.2. A peculiar morphology of X-ray emission is associated with radio and infrared flares. The X-ray emission changes from a high oscillating state (at a period of 10–20 s) to a low hard state (in a timescale of about 100 s). The X-ray intensity in the low hard state gradually increases. There is a sudden dip characterized by low intensity, low hardness ratio, and disappearance of the 0.5–10 Hz QPO. The source gradually returns to the high oscillating state. These are associated with the synchrotron flares in radio (Fender & Pooley 1998; Mirabel et al. 1998) and infrared (Eikenberry et al. 1998). The peak intensities of these flares are in the range $\sim$100–200 mJy from infrared to radio bands (Eikenberry et al. 2000). Eikenberry et al. (1998) strongly argue that the onset of radio/infrared flare is associated with the soft dip rather than the gradual change to the low hard state.

3.3. Eikenberry et al. (2000) identify a series of X-ray dips coincident with faint infrared flares. The peak amplitude of the observed mini-infrared flares is found to be $\sim$0.5 mJy for a duration of a few hundred seconds. The period of the soft X-ray dips, producing the observed flares, is found to be $\sim$20 s. These soft dips have the X-ray characteristics identical to the dips seen during the synchrotron infrared flares (3.2 above).

4. The huge radio flares producing superluminal blobs are associated with chaotic X-ray variability (as measured by low time-resolution X-ray data). The radio spectrum is steep during these flares. There is, as yet, no strong morphological identification with detailed X-ray emission characteristics.

In the following sections we argue that these soft X-ray dips are responsible for the superluminal radio flares.

4.2. *Radio Flare as a Collection of X-Ray Dips*

The peculiar dips presented in this paper provide an additional feature in the X-ray emission that, we argue, is related to mass ejection and the consequent jet production. There is a vast difference in the nature of the X-ray light curves of the source between the 1999 June observation reported in the present work and those seen in 1997 using PPCs (Paul et al. 1998; Yadav et al. 1999) and *RXTE* (Belloni et al. 1997). During the present observations the spectrum was softer as the hardness ratio of the source was less during the dips in comparison to the nondip regions. The observed properties of the source during the nondip periods, i.e., rms variability in X-ray flux and presence of QPO at a centroid frequency of 4–6 Hz, disappear during the dip. There is a gradual return to the accretion-disk properties; the hardness ratio and the variability characteristics slowly change back to the predip values (see Fig. 4).

Morphologically, these dips have properties very similar to those seen during the dips responsible for the infrared flares (Eikenberry et al. 1998, 2000; Mirabel et al. 1998). Fender et al. (1999) have worked back the onset time of the superluminal blobs, and during these times the radio emission shows oscillations in a timescale of 20–30 minutes. Similar radio oscillations (at similar periods but at lower intensity) are observed to be accompanied by a series of soft X-ray dips (see Fig. 10 of Dhawan et al. 2000). Further, one of the superluminal blobs was thought to originate from the core on MJD 50,750.5 (which is accompanied by radio oscillations), and the X-ray emission observed on MJD 50,751.7 shows soft X-ray dips (see Fig. 1*e* of Muno et al. 1999).

In view of strong evidence for association of such dip events to radio emission, it is suggested that a series of dips can produce the complete radio flare lasting for a few days. The onset of the first dip event detected with the PPCs on June 8, 15.51 UT and independently with the *RXTE* coincided with the onset of the radio flare within a few hours. It was shown in § 4.1 that a superposition of several disk-evacuation events can produce the radio flare if one assumes a scaling for energy from single-dip events. It would be interesting to see whether all radio flares are necessarily accompanied by such X-ray dips interpreted as disk-evacuation events.

To produce the observed radio light curve, one needs to assume that the number of dips produced as a function of time also follows a similar time profile. Since the IXAE data are obtained for only five of the 14 orbits every day, observations are not continuous enough to establish conclusively this hypothesis. It may be pointed out that during the superluminal jet events of 1997 October–November, the frequency of radio oscillations decreased from 2.9 hr^{-1} on MJD 50,750.5 (when the radio flux was 200 mJy) to 1.9 hr^{-1} on MJD 50,752.5 (when the radio flux decreased to 120 mJy; see Fig. 4 of Fender et al. 1999). The smooth radio light curve and the steep spectrum could be due to the movement of the ejecta in the interstellar medium. The radio flares of 1997 October–November seen by Fender et

al. (1999) are the superposition of at least four ejecta, and the start of each ejecta is associated with a series of radio oscillations.

The mass and energy estimates of the superluminal blobs emitted by GRS 1915+105 (Rodríguez & Mirabel 1999) are too large to be caused by a single isolated event in the accretion disk, and a series of accretion disk–driven events would be required, as suggested by Fender et al. (1999). The series of dips that we have observed could provide the necessary energy for the superluminal blobs if they occur in a rapid series. A continuous X-ray monitoring during a radio flare will clarify this question. Also, the dips seen during the later part of the radio flare are of shorter durations, and these events may not be ejecting matter in sufficient quantities. It is quite conceivable that only the long duration dips with a gradual recovery are responsible for jet emission. The start of the dips always shows similar observable parameters like count rates and hardness ratio, indicating a causal relationship between disk parameters and the onset of dip events.

4.3. *TCAF Model for the Advection Accretion*

We attempt to interpret the present results in light of the TCAF model for the advective accretion disk around the black holes. It has been recognized that very near to the black hole accretion is necessarily advective, and far away from the compact object it is believed that the accretion is through a geometrically thin accretion disk. In the advection-dominated accretion flow (ADAF) model of Narayan & Yi (1994) the changeover occurs at a transition radius ($r_{\rm tr}$), whereas in the TCAF model of Chakrabarti & Titarchuk (1995) a standing shock wave or a centrifugal barrier dominated dense region at R_0 separates these two. Das & Chakrabarti (1999) have included the effect of outflow in the TCAF model. GRS 1915+105 changes from hard to soft states at a variety of timescales, and the observed properties of the source can be interpreted as the variation in R_0.

4.3.1. *Timescales of the Dip Events*

Yadav et al. (1999) derived various timescales for the quiescent period, decay time, and rise time for the different types of bursts observed by equating the inner disk radius ($R_{\rm in}$) to R_0 from where the advection-dominated halo component covers the thin accretion disk during the quiescent state. They obtained the viscous timescale for the standard α disk ($t^d_{\rm vis}$) as

$$t^d_{\rm vis} = (4.3 \times 10^{-4})\alpha^{-1}\dot{m}_d^{-1}\, m^{-1} R_0^2 \,, \tag{4}$$

where $\dot{m}_d$ is in the unit of Eddington accretion rate, m is the mass of the source in the unit of solar mass, and R_0 is in km. They calculated this timescale ($t^d_{\rm vis}$) to be of the order a few hundred seconds for $\dot{m}_d = 1$, $m = 10$, $\alpha = 0.01$, and $R = 300$ km.

Similarly, the timescale for the advection disk for halo component $t^h_{\rm vis}$ (Yadav et al. 1999) is

$$t^h_{\rm vis} = (4.9 \times 10^{-6})\alpha^{-1} m^{-1/2} R_0^{3/2} \,. \tag{5}$$

Using the parameters used to derive $t^d_{\rm vis}$, the free-fall timescale is calculated to be of the order of seconds, which agrees with the decay time of the observed dips. The recovery time of the dips ($\sim$110 s) agrees with the calculated viscous timescale of the standard disk $t^d_{\rm vis}$.

The timescale of the dip onset (a few seconds) is comparable to the free-fall timescale as well as the advective disk timescale (eq. [5]) for typical advection-dominated disk parameters. Hence, we can conclude that all the accretion-disk characteristics suddenly disappear during the dips, and they reappear in a gradual way. We feel that a sudden disk evacuation and a gradual refilling is a natural explanation for this observation.

4.3.2. *TCAF Explanation for the Outflow*

To produce radio jets, a large amount of matter has to be expelled from the disk, and this has to be accelerated to relativistic velocities. Das & Chakrabarti (1999) have proposed a combined inflow/outflow model in which the computation is done using combinations of exact transonic inflow and outflow solutions; assuming free-falling conical polytropic inflow and isothermal outflows, they estimated the ratio of out flowing and inflowing rate to be

$$\frac{\dot{M}_\odot}{\dot{M}_{\rm in}} = R_{\dot{m}} = \frac{\Theta_{\rm out}}{\Theta_{\rm in}} \frac{R}{4}\, e^{-[f_0-(3/2)]} f_0^{3/2} \,, \tag{6}$$

where $\Theta_{\rm out}$ and $\Theta_{\rm in}$ are the solid angles of the outflow and inflow, respectively, R is the compression ratio of the inflowing matter, which is a function of the flow parameters such as specific energy and angular momentum (Chakrabarti 1990), and f_0 is given by

$$f_0 = \frac{R^2}{R-1} = \frac{(2n+1)R}{2n} \,, \tag{7}$$

where n is the polytropic constant $= 1/(\gamma - 1)$, γ being the adiabatic index.

They found that the outflow rate depends on the initial parameters of the flow, and in some cases the outflow rate can be higher than the inflow rate, leading to disk evacuation. We propose that the dips that we have observed are a result of such disk-evacuation phenomenon. It would be interesting to carry out a detailed spectral and timing analysis to extract the exact disk parameters leading to a disk-evacuation event.

4.4. *Jet Acceleration*

It is possible that the accretion-disk magnetic field is responsible for accelerating the disk-evacuated matter into radio-emitting jets. Meier et al. (1997) have proposed a magnetic switch that can generate superluminal jet ejection. They have shown that when the coronal Alfvén velocity exceeds a critical value, the jet velocity can become relativistic. We have calculated the Alfvén velocity by assuming the advection-dominated disk parameters given by Narayan, Mahadevan, & Quataert (1998).

The expression for Alfvén velocity ($V_{\rm A}$) and escape velocity ($V_{\rm esc}$) are

$$V_{\rm A} = \frac{B}{\sqrt{4\pi\rho}} \,, \tag{8}$$

$$V_{\rm esc} = \sqrt{\frac{2GM}{r}} = \frac{c}{\sqrt{r}} \,, \tag{9}$$

where B is the magnetic field, r is the radial distance, ρ is the plasma density, and r is the distance in the unit of Schwarzschild radius.

Assuming an equipartition with the magnetic energy, the expression for B and n_e (number density) are given by (Narayan et al. 1998)

$$B \simeq (7.8 \times 10^8)\alpha^{-1/2} m^{-1/2} \dot{m}^{1/2} r^{-5/4}\ {\rm G} \,, \tag{10}$$

$$n_e \simeq (6.3 \times 10^{19})\alpha^{-1}m^{-1}\dot{m}r^{-3/2}\ \mathrm{cm}^{-3}\ , \qquad (11)$$

where α is Shakura & Sunyaev viscosity parameter, m is in the unit of $M_\odot$, and $\dot{m}$ is in the unit of Eddington accretion rate.

For equipartition of magnetic field (i.e., $\beta = 0.5$), $\alpha = c(1-\beta) \simeq 0.3$ (for $c \sim 0.5$–0.6). Taking the values of m as 10 and $\dot{m}$ as 0.1–1 for GRS 1915+105, we estimated the magnetic field and the density (assuming one proton corresponding to one electron in the plasma) as

$$B = (4.51 \times 10^{8})\dot{m}^{1/2}r^{-5/4}\ \mathrm{G}$$
$$\rho = (3.5 \times 10^{-5})\dot{m}r^{-3/2}\ \mathrm{g\ cc}^{-1}\ .$$

Using the values of B and ρ, the Alfvén velocity V_A is calculated to be

$$V_A = \frac{B}{\sqrt{4\pi\rho}} = \frac{2.1 \times 10^{10}}{\sqrt{r}} \simeq \frac{2}{3}\frac{c}{\sqrt{r}}\ . \qquad (12)$$

Now, the ratio between V_A and V_{esc} is

$$\frac{V_A}{V_{esc}} = \frac{2}{3}\ . \qquad (13)$$

We find that the Alfvén velocity is near the critical velocity for advection-dominated flows, indicating the operation of the magnetic switch. It should be noted that just before the detection of the superluminal jet ejection in GRS 1915+105 in 1997 November by Fender et al. (1999), the source was in a low hard state as well as a radio-loud state. We can envisage a scenario where the accretion-disk condition during a low hard state makes the magnetic switch to operate and the ejected material is accelerated to relativistic velocities. These accelerated blobs can move in the interstellar medium to give the steep spectrum superluminal ejecta. The transition period from a low hard to a high soft state provides critical conditions for a series of disk-evacuation events to occur so that sufficient matter is ejected to produce relativistic jets. A continuous monitoring in X-ray and radio bands during a radio flare will clarify most of these questions.

We express sincere thanks to the referee for his or her useful comments and suggestions that improved the contents and presentations of the paper. We acknowledge the contributions of the scientific and technical staff of TIFR, ISAC, and ISTRAC for the successful fabrication, launch, and operation of the IXAE. It is a pleasure to acknowledge constant support of K. Thyagarajan, Project Director for the *IRS*-P3 satellite, J. D. Rao and his team at ISTRAC, P. S. Goel, Director ISAC and the Director of the ISTRAC. We thank the *RXTE*/ASM and NSF-NRAO-NASA Green Bank Interferometer group for making the data publicly available. The Green Bank Interferometer is a facility of the National Science Foundation operated by the NRAO in support of NASA High Energy Astrophysics programs.

REFERENCES

Agrawal, P. C., Paul, B., Rao, A. R., Vahia, M. N., Yadav, J. S., Marar, T. M. K., Seetha, S., & Kasturirangan, K. 1996, IAU Circ. 6488
Agrawal, P. C. 1998, in High Energy Astronomy and Astrophysics (Hyderabad: University Press), 408
Belloni, T., Mendez, M., King, A. R., van der Klis, M., & van Paradijs, J. 1997, ApJ, 479, L145
Castro-Tirado, A. J., Brandt, S., & Lund, N. 1992, IAU Circ. 5590
Chakrabarti, S. K. 1990, Theory of Transonic Astrophysical Flows (Singapore: World Scientific)
Chakrabarti, S. K., & Titarchuk, L. G. 1995, ApJ, 455, 623
Chen, X., Swank, J. H., & Taam, R. E. 1997, ApJ, 477, L41
Das, T. K., & Chakrabarti, S. K. 1999, Classical Quantum Gravity, 16, 3879
Dhawan, V., Mirabel, I. F., & Rodríguez, L. F. 2000, ApJ, 543, 373
Eikenberry, S. S., Matthews, K., Morgan, E. H., Remillard, R. A., & Nelson, R. W. 1998, ApJ, 494, L61
Eikenberry, S. S., Matthews, K., Muno, M., Blanco, P. R., Morgan, E. H., & Remillard, R. A. 2000, ApJL, 532, L33
Fender, R. P., Garrington, S. T., McKay, D. J., Muxlow, T. W. B., Pooley, G. G., Spencer, R. E., Stirling, A. M., & Waltman, E. B. 1999, MNRAS, 304, 865
Fender, R. P., & Pooley, G. G. 1998, MNRAS, 300, 573
Feroci, M., Matt, G., Pooley, G., Costa, E., Tavani, M., & Belloni, T. 1999, A&A, 351, 985
Harmon, B. A., Deal, K. J., Paciesas, W. S., Zhang, S. N., Robinson, C. R., Gerard, E., Rodríguez, L. F., & Mirabel, I. F. 1997, ApJ, 477, L85
Markwardt, C. B., Swank, J. H., & Taam, R. E. 1999, ApJ, 513, L37
Meier, D. L., Edington, S., Godon, P., Payne, D. G., & Lind, K. R. 1997, Nature, 388, 350
Mirabel, I. F., Dhawan, V., Chaty, S., Rodríguez, L. F., Marti, J., Robinson, C. R., Swank, J., & Geballe, T. 1998, A&A, 330, L9
Mirabel, I. F., & Rodríguez, L. F. 1994, Nature, 371, 46
Morgan, E. H., & Remillard, R. A. 1996, IAU Circ. 6392
Muno, M. P., Morgan, E. H., & Remillard, R. A. 1999, ApJ, 527, 321
Narayan, R., Mahadevan, R., & Quataert, E. 1998, in The Theory of Black Hole Accretion Discs, ed. M. A. Abramowicz, G. Bjornsson, & J. E. Pringle (Cambridge: Cambridge Univ. Press), 148
Narayan, R., & Yi, I. 1994, ApJ, 428, L13
Paul, B., Agrawal, P. C., Rao, A. R., Vahia, M. N., Yadav, J. S., Seetha, S., & Kasturirangan, K. 1998, ApJ, 492, L63
Rao, A. R., Agrawal, P. C., Paul, B., Vahia, M. N., Yadav, J. S., Marar, T. M. K., Seetha, S., & Kasturirangan, K. 1998, A&A, 330, 181
Rodríguez, L. F., & Mirabel, I. F. 1999, ApJ, 511, 398
Trudolyubov, S., Churazov, E., & Gilfanov, M. 1999, Astron. Lett., 25, 718
van der Laan, H. 1966, Nature, 211, 1131
Yadav, J. S., Rao, A. R., Agrawal, P. C., Paul, B., Seetha, S., & Kasturirangan, K. 1999, ApJ, 517, 935